



Effect of Post Weld Heat Treatment on Donor Material Assisted Friction Stir Welding of AA6061-T6 Alloy on Microstructure and Mechanical Properties

Srinivasa Bhukya¹, Zhenhua Wu¹(✉), and Abdelmageed Elmustafa²

¹ Department of Engineering, Virginia State University, Petersburg, VA 23806, USA
zwu@vsu.edu

² Department of Mechanical and Aerospace Engineering, Old Dominion University, Norfolk, VA 23529, USA

Abstract. In this study, the influence of post weld heat treatment (PWHT) on the microstructure and mechanical properties of a copper (Cu) donor material assisted friction stir welding (FSW) of AA6061-T6 aluminum alloy has been investigated. Cu assisted FSW joints of AA6061-T6 alloy were prepared at an optimized constant tool rotational rate of 1400 rpm and welding speed at 1 mm/s. The Cu donor material of 20% thickness with respect to the workpiece thickness was selected to assist the FSW joining at the plunge stage. FSWed AA6061-T6 samples were prepared using solid solution treatment at 540 °C for 1 hour followed by quenching in water at room temperature. It was then artificially aged at 180 °C for 6 hours and 24 hours followed by air cooling. The microstructure and tensile fractured surfaces were analyzed using scanning electron microscope and optical microscope. The microstructure depicts an additional grain refinement in the stir zone (SZ) due to the occurrence of recovery and recrystallization with increasing aging time. Vickers micro hardness indicates a softening effect due to the dissolution of hardening precipitates. Hardness recovery is most likely attributed to the uniform distribution of fine hardening precipitates at all aging time levels. The maximum hardness was 92.5 HV at the SZ and the tensile properties were significantly improved by 20 % after solution heat treated at 540 °C for 1 hour followed by artificial aging at 180 °C for 24 hours.

Keywords: Al6061-T6 alloy · Cu donor material · Friction stir welding · Heat treatment microstructure · Micro-hardness · Tensile properties · Fractography

1 Introduction

Defense industries have particular interest in processing lightweight materials. Aluminum alloys (AA) are essential light-weight materials in a variety of military applications due to their higher strength-to-weight ratio compared to steels. They also cost less than other light-weight alloys such as titanium or magnesium alloys. AA5083, 2139, and 7039 series alloys are often applied on armored vehicles [1]. These grades meet

the military requirements on projectile resistance, corrosion resistance, lightweight, and weldability. Ballistic and armor piercing tests will be performed on aluminum armor plates to ensure the strength and safety for military applications. Although these alloys are being applied on military applications, the complexity in manufacturability and sustainment of selecting aluminum alloys for vehicle hull structures increased due to lack of better welding techniques. These aluminum alloys usually perform poor weldability in conventional fusion welding. As an alternative, friction stir welding (FSW), a solid state welding process, is a promising alternative for welding aluminum alloys on overcoming defects such as porosities, solidification cracking, high residual stress etc., which are generally associated with fusion welding processes [2]. FSW has been widely utilized in defense and aerospace structural applications. Although FSW possesses the capability to produce good quality welds and to lower cost compared to other welding processes, the strength loss at the weld zones due to heat generation is still a major concern [3–5]. Typically, after the welding takes place, the base metal loses its strength due to high temperature during the welding process [6]. For example, welds strength and elongation of gas metal arc welded (GMAWed) AA2139-T8 are only 35–55% of the base material. To strengthen the aluminum alloy weldments, solution heat treatment followed by rapid water quenching, and precipitation heat treatment should be performed. This solution heat treatment process results in a metallurgical structure within the alloy that enhances the strength of the material [7]. The formation of precipitation and distribution depends on solution treatment temperature and artificial aging time levels. The main precipitation in the 6000 series aluminum alloy is Mg_2Si because silicon (Si) and magnesium (Mg) are the two major alloying elements, which are typically added in the proportions required for the formation of hardening precipitates of Mg_2Si , thus rendering them heat treatment by solutionizing and artificial aging processes.

Heat treatment changes the internal microstructure to achieve the desired mechanical properties including hardness, ultimate tensile strength, and corrosive resistance, etc. For this purpose, these alloys are processed via various heat treatment approaches, by altering the solutionizing temperatures and at different aging time levels [8]. Several manufacturing industries are following the ASTM B917 and ASTM B91 standards for precipitation hardening or called as T6 heat treatment, which involves a solution heat treatment at a temperature of 540 °C, with a residence duration between 6–12 hours, followed by artificially aging at 155 °C between 3–5 hours [9]. Rosso and Actis have suggested that solutionizing a metal for 1 hour rather than 6 hours would yield significantly better tensile strength and further subjecting the metal to 180 °C for 4 hours by artificial aging can yield better mechanical properties [10]. Shivkumar et al. [11] and Zhang et al. [12] concluded that the solution heat treatment temperature of 540 °C was sufficient followed by artificial aging time between 3–5 hours at 155 °C can yield better hardness and strength.

Researchers have worked on post weld heat treatment (PWHT) of FSWed AA6061-T6 alloy for aerospace industry applications. The weldment strength was increased considerably by precipitation through solid solution treatment and artificial aging processes. Cabibbo et al. [13] studied the effect of PWHT on FSW of AA6056 and reported considerable increment of tensile strength due to formation of high density precipitation of Mg_2Si . El-Danaf and El-Rayes [14] studied the effect of PWHT on FSW of AA6082 at

175°C for 5 hours and 12 hours. Jamshidi and Serajzadeh [15] also reported that artificial aging increased the hardness of the FSWed AA6061 alloy. Sato et al. [16] investigated the formation of precipitates in FSW of AA6063 alloy by artificial aging process. Although the formation of fine recrystallized grains, the dissolution and growth of precipitates were noticed in the weld zone subsequent to FSW. By applying aging, it was found that hardening precipitates reformed, leading to a full recovery of the mechanical properties. Previous studies indicate the post artificial aging is necessary to achieve sufficient strength and hardness at the weld zone of a friction stir processing of 6000 series aluminum alloys. Priya et al. [17] investigated the PWHT on FSW AA6061-T6 and AA 2219-T6 alloy, and concluded that the ultimate tensile strength was increased due to the presence of fine precipitated particles. Hu et al [18] performed PWHT of a friction stir welded AA2024, and reported that the mechanical properties did not change but elongation of welds was increased. Aydin et al. [19] studied the solution heat treatment followed by ageing process on friction stir welded AA2024-T6 alloy, the mechanical properties increased at 190 °C for 10h artificial ageing compared to natural ageing. Bhukya et al. [20] recently reported the effects of copper donor material assisted FSW of AA6061-T6 alloy on microstructure and mechanical properties, but not on PWHT. The effect of PWHT on Cu donor material assisted FSW of AA6061-T6 has not been investigated. Therefore, in this study, we investigate post weld mechanical properties (tensile, micro-hardness) of solid solution heat treatment of 1 hour at 540 °C, followed by artificial aging of 0, 6, and 24 hours at 180 °C. The fracture mechanisms were also evaluated using field emission scanning electron microscopy.

2 Experimental Procedure

The procedure to prepare the Cu donor material assisted FSW can be referred to [20]. The base metal used in this study was extruded AA6061-T6 in sheets with dimensions 6.35 mm (thickness) × 304.8 mm (length) × 76.2 mm (width). The chemical composition and mechanical properties of AA6061-T6 aluminum alloys are listed in Tables 1 and 2 respectively. Test coupons, with dimensions of 152.4 mm (length) × 76.2 mm (width), were sectioned from the as-received sheets followed by milling of the edges along the length. Pockets on workpiece for embedding donor material have a dimension of 63.5 mm (length) × 25.4 mm (width). The pockets and donor piece were cut using a CNC mill before the welding. The selected Cu donor material thickness for the investigation was 20% the workpiece thickness. FSW was conducted in the position control mode with a triangle tapered pin-type tool made of H13 steel. The tool is consisted of a shoulder with a diameter of 15.8 mm and an adjustable 1/2- 16 left-hand threaded pin having a diameter of 6.4 mm, a threaded length of 6.35 mm, a 60° thread form at 1 mm pitch and 0.4 mm deep (normal to the surface). The tilted angle was maintained at 2° with a shoulder heel plunge depth (the portion of the shoulder under the top surface of the workpiece) of approximately 0.5 mm for all the welding experiments. The welding direction was parallel to the extruded direction of the workpiece as shown in Fig. 1 in reference [20]. All the joints were friction stir butt-welded at a welding speed of 1mm/s and tool rotation of 1400 rpm. It is noted that relative to the welding and tool rotational directions as indicated in Fig. 1 in reference [20], the welds were manufactured with the tool rotating counter clockwise.

Table 1. Chemical composition of AL6061-T6 and Cu 110 alloys.

Components		Al	Cr	Cu	Fe	Mg	Mn	Ni	Si
Alloy	Al6061-T6	95.1-98.2	0.4-0.8	0.05-0.4	0-0.7	0.8-1.2	0.0-0.15	0.0-0.05	0.4-0.8
	Cu 110	-	-	99.9	-	-	-	-	-
Components		Ti	Zn	Zr	Bi	Pb	O	Others	
Alloy	Al6061-T6	0.0-0.15	0.0-0.25	0.0-0.25	-	-	-	-	0.15
	Cu 110	-	-	-	0.0-0.005	0.0-0.005	0.0-0.04	-	-

Table 2. Mechanical properties of Cu 110 and Al6061-T6.

Materials	Hardness (Rockwell)	Yield strength, MPa	UTS, MPa	Thermal conductivity, W/mK	Melting Point, °C
Copper 110	55	255	345	183	1084
Al6061-T6	40 (scale A), 60 (scale B)	241	262	151	585

To investigate the influence of PWHT on mechanical properties, the weldments were divided into two groups, namely As-Welded (AW) and heat treated samples. The heat treatment process included furnace solution treatment at a temperature of 540 °C for 1 hour, followed by immediate water quenching. The samples were then artificially aged inside the furnace at a temperature of 180 °C for 0, 6, and 24 hours as shown in Fig. 1. Heat treated metallography samples were then cold mounted, ground, polished, and etched with Keller’s reagent for approximately 120 seconds to reveal the grain structure. The metallographic analyses were conducted using Olympus optical microscopy equipped with quantitative image analysis software for microstructure and macrostructure studies, respectively. The effect of PWHT was characterized in terms of microstructure, Vickers micro-hardness, tensile test, and fractography. Using a wire electrical discharge machine (WEDM), the FSWed coupons were sectioned in the direction perpendicular to the welding direction (WD) to examine the microstructures in the weld cross-sections.

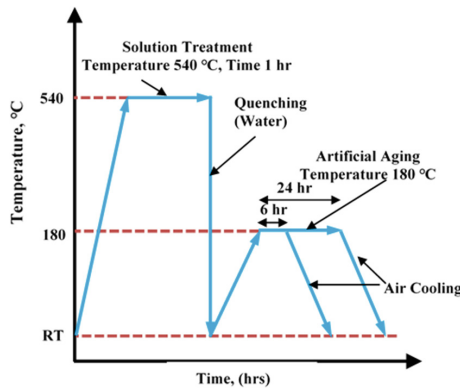


Fig. 1. Thermal cycle graph for solution treatment and artificial aging heat treatment process.

Automated Vickers micro-hardness measurements were conducted across the butt welds using a load of 100 g, a dwell time of 15 s, and an indent interval of 0.3 mm (i.e., at least three times the diagonal length of the indentation to prevent any potential effect of the strain fields caused by adjacent indentations). The tensile tests experiments were carried out on heat treated samples by a universal tensile testing machine (INSTRON-5869) with a 50kN load capacity. At least two samples were tested at each welding

condition. Tensile samples were prepared according to ASTM E8/E8M-13a [21]. All tensile tests were performed up to failure at room temperature and at a crosshead speed of 1.5 mm/min. The fractured surface of the frictionally stir welded (FSWed) samples subsequent to the tensile testing was examined using a JEOL 6700 field effect-scanning electron microscope (FE-SEM) equipped with three-dimensional (3-D) fractographic analysis capacity.

3 Results and Discussion

3.1 Microstructure

Figure 2(a–d) shows the microstructure from AW condition to PWHT at different aging time obtained at the SZ location. Microstructure in the SZ is composed of grains with slightly uneven boundaries, this could be due to high plastic deformation during FSW process. Also during FSW, the dissolution of strengthening particles in the SZ was significant in the T6-treated base plate microstructure.

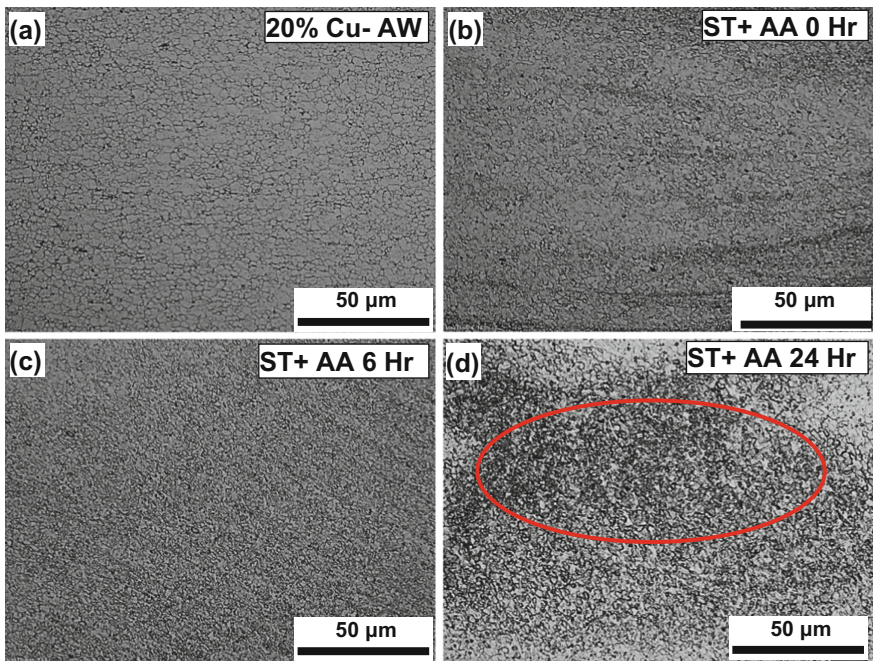


Fig. 2. Optical microstructure images after PWHT at SZ of joints made at 20% Cu, 1400 rpm and 1 mm/s, a) 20% Cu A, b) ST+AA 0Hr, c) ST+ AA 6 Hr, and d) ST+ AA 24 Hr.

PWHT resulted in the precipitation of strengthening particles in the SZ of all the joints produced as shown in Figs. 2(d) and 3(b). The grain size decreased with increasing aging time as shown in Fig. 2(a–d). It was also noticed that after PWHT, significant amount

of small circular black particles were noticed on the surface of the specimens as shown in Fig. 2(d), which was less visible in the AW samples, Fig. 2(a). These small particles popped out after PWHT because PWHT samples have a better strength than the AW samples due to the presence of Mg_2Si intermetallic particles [19]. Generally, this type of particles can be found in AA6061-T6 alloy when the material undergoes heat treatment followed by artificial aging process. These particles became more and more aggressive when the aging time increased to 24 hours. The grain size was observed to be finer and equiaxed as the time of aging increased for all PWHT joints. Figures 3(a–b) show the SEM images of before and after PWHT on the 20% Cu samples. In addition, the density of these precipitations of small black particles are remarkably increased with increasing aging condition. The precipitation microstructure of Mg_2Si during aging for AA 6061-T6 alloys is well known in the literature [22–24].

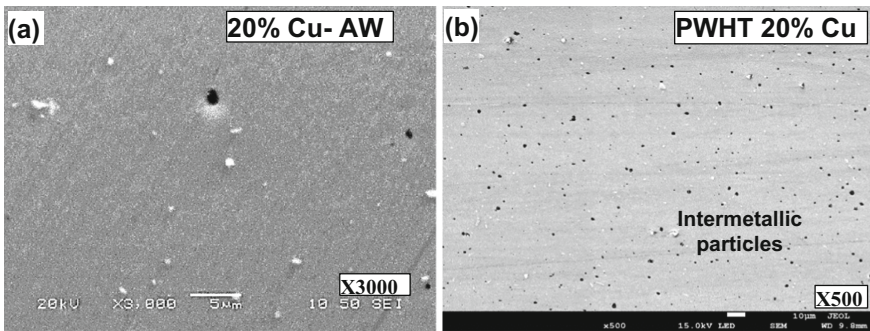


Fig. 3. Typical SEM images of a) as welded, and b) PWHT samples, with 20% Cu donor material assisted FSW at a rotational rate of 1400 rpm and a welding speed of 1 mm/s

3.2 Micro-hardness

Figure 4 shows the Vickers micro-hardness profiles obtained at the center of the workpiece across the weldments at 1400 rpm and 1 mm/s welding condition. The indentation hardness is measured starting from the base metal (BM) advancing side (AS) to the BM retreating side (RS). It was observed that the hardness profiles exhibited a W-shape with the softening area containing the nugget zone in the weld center and the TMAZ beside the nugget zone for the AW and AW 20% Cu samples, whereas the hardness profiles for the PWHT samples at each specific artificial aging conditions are almost flat with some increment at the SZ.

From the plotted hardness profiles in Fig. 4, it was noticed that the RS of the weld closer to the tool pin had lower hardness compared to the AS of the weld, this is due to strains developed in the workpiece by the welding tool. The temperature during FSW on the AS side is higher than on the RS side, which enhances the hardness on the AS side. It was observed that at the stir zone after PWHT for 24 hours artificial aging condition had higher hardness than AW for all weld regions, hardness recovery is most likely attributed to the uniform distribution of fine hardening precipitates at all aging times. In addition,

the aging time had a significant effect on the hardness of a weld, while the hardness increased significantly at the center of the weld, i.e., at the SZ region from 59.2 to 92.4 HV with an increase in aging time from 6 to 24 hours. The reason behind increasing the hardness at the SZ is due to the presence of strengthening particles which can be seen in Figs. 2(d) and 3(b).

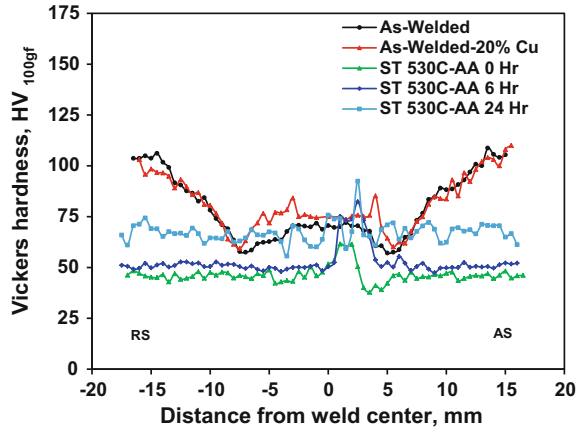


Fig. 4. Micro-hardness profiles of a PWHT FSW joints made at a) 20% Cu, 1400 rpm and 1 mm/s of an as-welded and heat treated samples.

3.3 Tensile test

Figure 5(a) shows the comparison of tensile test properties of joints made at optimized process parameters of 1400 rpm tool rotational speed and 1 mm/s welding speed. The ultimate tensile strength (UTS) of the Cu donor material assisted FSWed AA6061-T6 samples were found to be less than the base material. The average UTS for AW samples was 192 MPa. It was noticed that, using the same tool rotational and welding speeds, the average UTS of the 20% Cu donor assisted FSW joints were similar to the AW samples of ~190 MPa. For the PWHT joints, the average UTS increased significantly to 230 MPa for the artificial aging of 24 hours, which is improved by approximately 20%, while the UTS values were 162 and 120 MPa for the 6 hours and 0 hour of a Cu donor assisted samples respectively. The precipitation of intermetallic particles was visible for PWHT samples at for the 24 hours condition and can be seen clearly in Fig. 2(d). It was also observed that the ductility and elongation decreased constantly with the increase in the time of aging. This improvement in the strength of PWHT is due to uniform precipitation throughout the weld [17]. The change in fracture and microstructure morphologies had a significant effect on the mechanical properties of AA6061.

Figure 5(b) shows the comparison of ultimate tensile strength (UTS), elongation, and joint efficiency (UTS welded joint/UTS unwelded joint). The elongation decreases by increasing the artificial aging and the joint efficiency significantly improved from ~73 to ~88% after PWHT at 24 hours of artificial aging. This could be due to the appearance of strengthening particles after PWHT.

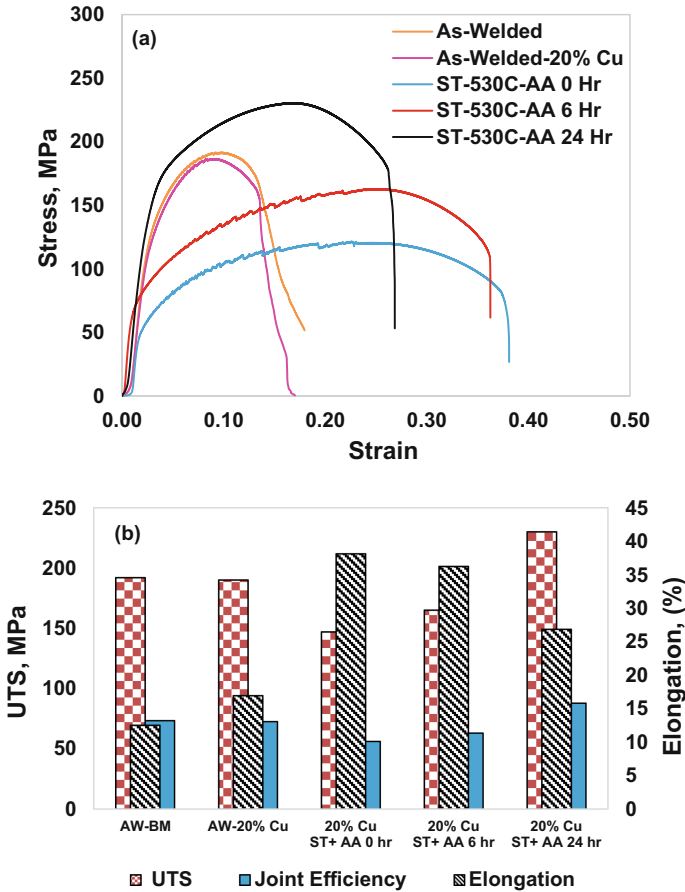


Fig. 5. Tensile test plots of with and without donor material at a constant 530 °C solution treatment and 0 hour, 6 hours, and 24 hours artificial aging time levels at 180 °C.

3.4 Fractography

Fractured surfaces of all tensile samples were investigated by FE-SEM at different locations as shown in Fig. 6(a–d). All the fracture morphologies were taken at 1400 rpm and 1 mm/s welded samples. It has been observed that crack initiation occurs near the TMAZ/HAZ on the RS even after PWHT. The fractured surface presents large number of small spherical dimples with layered distribution, which is often in a ductile fracture. The 20% Cu donor material AW condition samples exhibit intergranular cracking with coarser dimples. These type of dimples appear in ductile fractured surfaces, which generally corresponds to voids generated during testing. For every PWHT joint, the dimples were becoming finer and the grains that emerged were smaller than AW as the time of aging increased. The dislocation between the grains, and the grain size as well as distribution of grains play a major role in the mechanical properties such as tensile

strength and hardness values. These are the reasons for the higher tensile strength and improvement in hardness values for the PWHT samples.

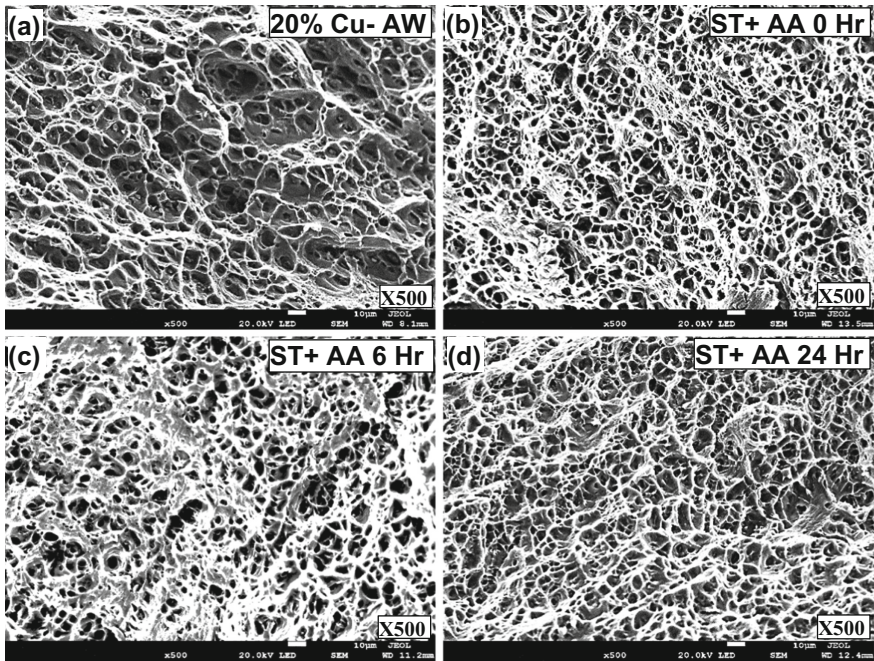


Fig. 6. Typical SEM tensile tested fracture surface images of a PWHTed samples with 20% Cu donor material at a rotational rate of 1400 rpm and a welding speed of 1 mm/s.

4 Conclusions

In this study, the microstructure and mechanical properties of weld joints after PWHT were studied on a 20% Cu donor material assisted FSW samples. The following important conclusions are drawn from this study.

- The stir zone (SZ) and the thermo-mechanically affected zone (TMAZ), which were predominantly composed of equiaxed grains, experienced full dynamic recrystallization. The grain size in the SZ became very much finer after PWHT followed by 24 hours artificial aging process. Significant amount of strengthening intermetallic particles of Mg_2Si were observed after PWHT which changed the structure of AA6061-T6 alloy.
- Before heat-treatment, the joints exhibited a W-shaped hardness profiles as seen in the cross-section. After PWHT the hardness profiles were flatter with sudden increment at the center of the weld. The minimum measured hardness was HV 80–85 for AW condition while the minimum hardness was HV 85–92 for PWHT condition.

- The hardness value increased by 10% after PWHT and the overall measured hardness across the SZ was slightly higher at the advancing side of the weld due to higher heat input during the welding process.
- The maximum tensile strength obtained was 192 MPa for both with and without Cu donor material whereas, for the joints after PWHT, the tensile strength was 230 MPa which constitutes a significant improvement in the measurement of the UTS. This significant improvement is due to structural changes and its intermetallic particles. The tensile properties were significantly improved by 20% after solution heat treatment at 540 °C for 1 hour followed by artificial aging at 180 °C for 24 hours.
- Fractography of the AW tensile testing failure samples, AW condition samples exhibit intergranular cracking with large dimples. The fractured surface for PWHT samples appeared to be ductile like fracture with huge number of fine dimples. These type of dimples appear in the ductile fractured surface, which are only corresponding to voids. For every PWHT joint, the dimples were becoming finer and the grains that emerged were smaller than AW as the time of aging increased.

Acknowledgements. The authors would like to acknowledge support from NASA (award number: 80NSSC20M0015). The author ZW also acknowledges support from ONR (award number: N00014-19-1-2728). Any opinions, findings, and conclusions or recommendations expressed in this material are those of the author(s) and do not necessarily reflect the views of the NASA and ONR. The authors would also like to thank the Commonwealth Center for Advanced Manufacturing (CCAM) and Amsted Rail for providing the facility for sample characterization. The assistance of Mr. Geoff Widman in performing the experiments is also gratefully acknowledged.

References

1. Grujicic, M., Arakere, G., Pandurangan, B., Hariharan, A., Yen, C.-F., Cheeseman, B.A.: Development of a robust and cost-effective friction stir welding process for use in advanced military vehicles. *J. Mater. Eng. Perform.* **20**(1), 11–23 (2011)
2. Thomas, W.M., Nicholas, E.D., Needham, J.C., Murch, M.G., Templesmith, P., Dawes, C.J.: Patent Application No. 9125978.8 (1991)
3. Kallee, S.W.: Friction stir welding at TWI. The Welding Institute (TWI), Cambridge (2006)
4. Thomas, W.M., Dolby, R.E.: Friction stir welding developments. In: 6th International Proceedings of Trends in Welding Research, pp. 203–211. ASM International, Materials Park (2003)
5. Jata, V., Semiatin, S.L.: Continuous dynamic recrystallization during friction stir welding of high strength aluminum alloys. *Scripta Materialia* **43**(8), 743–749 (2000)
6. Lakshminarayanan, A., Balasubramanian, V.: Process parameters optimization for friction stir welding of RDE-40 aluminium alloy using Taguchi technique. *Trans. Nonferrous Met. Soc. China* **8**, 548–554 (2008)
7. Rudnev, V., Loveless, D., Cook, R.L., Black, M.: Handbook of Induction Heating. CRC Press (2002)
8. ASM Specialty Handbook: Aluminium and Aluminium Alloys. ASM International, Materials Park, Ohio, pp. 315–316 (1993)
9. Menargues, S., Martin, E., Baile, M.T., Picas, J.A.: New short T6 heat treatments for aluminium silicon alloys obtained by semisolid forming. *Mater. Sci. Eng. A* **621**, 236–242 (2015)

10. Rosso, M., Actis, G.M.: Optimization of heat treatment cycle for automotive parts produced by rheocasting. *Process Solid State Phenom.* **116–117**, 505–508 (2006)
11. Shivkumar, S., Ricci, S., Steenhoff, B., Apelian, D., Sigworth, G.: An experimental study to optimize the heat treatment of A356 Alloy. *AFS Trans.* **38**, 791–810 (1989)
12. Zhang, D.L., Zheng, L.: The quench sensitivity of cast Al7wt%Si0.4wt%Mg alloy. *Metall. Mater. Trans. A* **27**, 3983–3991 (1996)
13. Cabibbo, M., McQueen, H.J., Evangelista, E., Spigarelli, S., Di Paola, M., Falchero, A.: Microstructure and mechanical property studies of AA6056 friction stir welded plate. *Mater. Sci. Eng. A* **460**, 86–94 (2007)
14. El-Danaf, E.A., El-Rayes, M.M.: Microstructure and mechanical properties of friction stir welded 6082 AA in as welded and post weld heat treated conditions. *Mater. Des.* **46**, 561–572 (2013)
15. Jamshidi Aval, H., Serajzadeh, S.: A study on natural aging behavior and mechanical properties of friction stir-welded AA6061-T6 plates. *Int. J. Adv. Manuf. Technol.* **71**(5–8), 933–941 (2013). <https://doi.org/10.1007/s00170-013-5531-7>
16. Sato, Y.S., Kokawa, H., Enomoto, M., Jogan, S.: Microstructural evolution of 6063 aluminum during friction-stir welding. *Metall. Mater. Trans. A* **30**, 2429–2437 (1999)
17. Priya, R., Sarma, V.S., Rao, K.P.: Effect of post weld heat treatment on the microstructure and tensile properties of dissimilar friction stir welded AA 2219 and AA 6061 alloys. *Trans. Indian Inst. Met.* **62**, 11–19 (2009)
18. Hu, Z., Yuan, S., Wang, X., Liu, G., Huang, Y.: Effect of post-weld heat treatment on the microstructure and plastic deformation behavior of friction stir welded 2024. *Mater. Des.* **32**, 5055–5060 (2011)
19. Aydın, H., Bayram, A., Durgun, I.: The effect of post-weld heat treatment on the mechanical properties of 2024–T4 friction stir-welded joints. *Mater. Des.* **31**, 2568–2577 (2010)
20. Bhukya, S.N., Wu, Z., Maniscalco, J., Elmustafa, A.: Effect of copper donor material-assisted friction stir welding of AA6061-T6 alloy on downward force, microstructure, and mechanical properties. *Int. J. Adv. Manuf. Technol.* **119**, 2847–2862 (2022)
21. ASTM E8/E8M-13a: Standard test methods for tension testing of metallic materials. ASTM International, West Conshohocken (2013)
22. Osten, J., Milkereit, B., Schick, C., Kessler, O.: Dissolution and precipitation behaviour during continuous heating of Al–Mg–Si alloys in a wide range of heating rates. *Materials* **8**, 2830–2848 (2015)
23. Edwards, G.A., Stiller, K., Dunlop, G.L., Couper, M.J.: The precipitation sequence in Al–Mg–Si alloys. *Acta Materialia* **46**, 3893–3904 (1998)
24. Ozturk, F., Sisman, A., Toros, S., Kilic, S., Picu, C.: Influence of aging treatment on mechanical properties of 6061 aluminum alloy. *Mater. Des.* **31**, 972–975 (2015)